

Mechanism of the Oxidation of Iron

Minghuan Zhang^{1,a}, Qing Shao^{2,b}, Lu Yuan^{3,c}, Guangwen Zhou^{3,d},

Yiqian Wang^{1,e}

¹ College of Chemistry, Chemical Engineering and Environmental Engineering, Qingdao University,
No. 308 Ningxia Road, Qingdao, 266071, P. R. China

² College of Physical Science, Qingdao University, No. 308 Ningxia Road, Qingdao, 266071, P. R.
China

³ Department of Mechanical Engineering & Multidisciplinary Program in Materials Science and
Engineering, State University of New York, Binghamton, NY 13902, USA

^azhangminghuan@126.com, ^bshaoqing1992@163.com, ^clyuan1@binghamton.edu,
^dgzhou@binghamton.edu, ^eyqwang@qdu.edu.cn

Keywords: Oxidation Mechanism, Iron, TEM, SAED

Abstract. A layered structure of different iron oxides was produced by thermal oxidation of iron. The structure and microstructure of different layers were examined using scanning electron microscopy (SEM) and transmission electron microscopy (TEM). Selected area electron diffraction (SAED) was used to identify the structures of the different oxide layers. Two different structures of Fe₂O₃ were found to co-exist. Based on our observation, a possible oxidation mechanism for iron was proposed. The results shed light on the oxidation process of metals and provide insight into the synthesis of iron oxides.

Introduction

Significant research work has been focused on iron and iron oxides because of their wide applications. For example, hematite (Fe₂O₃) has good semiconducting properties because of its lower band gap (2.1eV) and is widely used as catalyst [1], gas sensing material [2] and pigments [3]. Magnetite (Fe₃O₄) is usually used in the field of magnetic recording media and some medical fields depending on its excellent magnetic properties [4]. The process of oxidation of iron has attracted great attention to form various iron oxides. However, cross-sectional TEM study of oxidation of Fe has been still few due to the challenge in preparing cross-sectional TEM samples and the magnetism issue of iron oxides for TEM imaging. In this paper, we investigate this process directly using SEM and TEM and propose an oxidation mechanism on the basis of the observation.

Experimental details

First, the high-purity (99.99%) iron foils were thoroughly rinsed with deionized water followed by ultrasonication in acetone for 5 min. Then, the cleaned iron substrates were put on a substrate heater in the vacuum chamber, and the temperature was monitored using a K-type thermocouple in contact with the heater. The chamber was pumped to a vacuum of about 2×10⁻⁶ Torr, and then filled with 200 Torr oxygen (oxygen purity: 99.999%). Subsequently, the chamber was sealed, and the iron foil was heated to 600°C at a rate of 20°C /min in the oxygen gas. After the

iron foil was oxidized for 1 h, it was then cooled down in the same oxygen atmosphere to room temperature at a rate of ~ 10 °C /min. Morphology and chemical composition of the oxidized samples were investigated using a field emission gun-scanning electron microscope (FEG SEM) FEI Supra 55VP. Cross-sectional specimens of the oxidized iron foil for transmission electron microscopy (TEM) observations were prepared using conventional techniques of mechanical polishing and ion-thinning. The ion-thinning was carried out using Gatan model 691 precision ion polishing system (PIPS). Selected-area electron diffraction (SAED) were carried out using a JEOL JEM 2100F TEM operated at 200 kV.

Results and Discussion

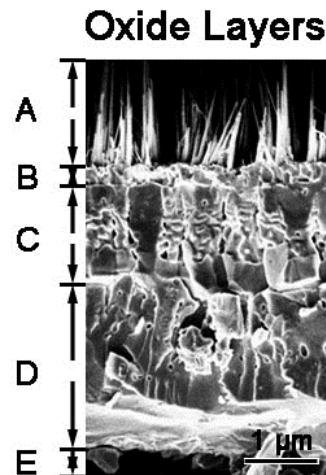


Fig.1 Cross-sectional SEM image of different oxide layers of iron oxidized at 600°C

Fig.1 shows a representative cross-sectional SEM image of oxidized iron foil. It can be seen that there are four different layers from the substrate to the surface. Part A is on the top of the surface, which is composed of many nanowires growing from layer B. The thickness of layer B is just about $0.3\mu\text{m}$. It is noticed that the composition of layer C are more regular but those of layer D are more disordered. Additionally, the thickness of layer D is larger than others and it's about $3\mu\text{m}$. To identify the crystal structure of the different oxide layers, TEM observations and SAED patterns were used in the following analysis.

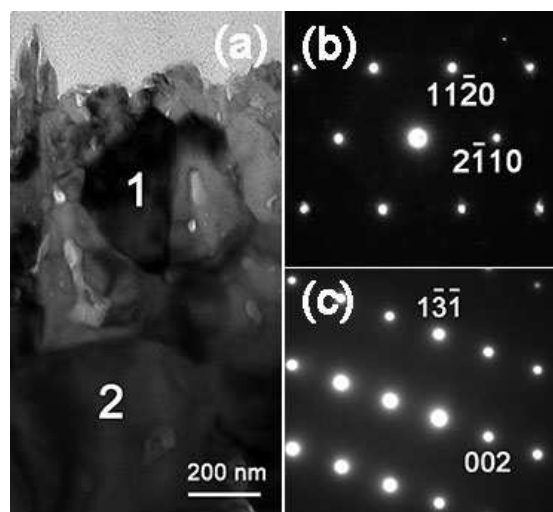


Fig.2 (a) Cross-sectional TEM image showing B, C parts of the Fig.1; (b) SAED pattern taken from grain 1 of (a); (c) SEAD pattern taken from grain 2 of (a)

Fig.2a is a cross-sectional TEM image which shows layers B, C of the Fig.1. From this image, it can be seen that the size of grain 1 is smaller than grain 2. The SAED patterns (b) and (c) are corresponding to grain 1 and grain 2 marked in Fig.2a, respectively. Fig.2b shows a typical [0001] zone-axis selected area electron diffraction (SAED) pattern taken from grain 1 and the diffraction pattern can be indexed with the α -Fe₂O₃ structure ($a=0.5034\text{nm}$, $c=1.375\text{nm}$). Meanwhile, the SAED pattern (c) can be indexed with the Fe₃O₄ structure ($a=0.839\text{nm}$), which is taken along [310] zone-axis of grain 2. On the basis of the analysis, it is revealed that layer B is α -Fe₂O₃ while layer C is Fe₃O₄.

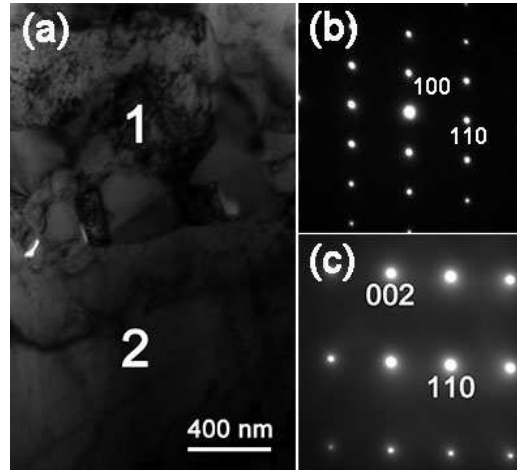


Fig.3 (a) Cross-sectional TEM image showing layer D and E of Fig.1; (b) and (c) SAED patterns corresponding to Part 1 and 2 of (a).

A cross-sectional TEM image showing layers D, E of Fig.1 is also presented as Fig.3a. The SAED patterns (b) and (c) are corresponding to Fig.3a 1 and 2, respectively. Fig.3b shows a typical SAED pattern taken along [001] zone axis of part 1 and the diffraction pattern is indexed with the FeO structure. The SAED pattern Fig.3c can be indexed with the Fe structure ($a=0.287\text{nm}$), which is taken along $[\bar{1}10]$ zone axis of part 2. In fact, layer E is iron substrate, which is identical to the SAED pattern.

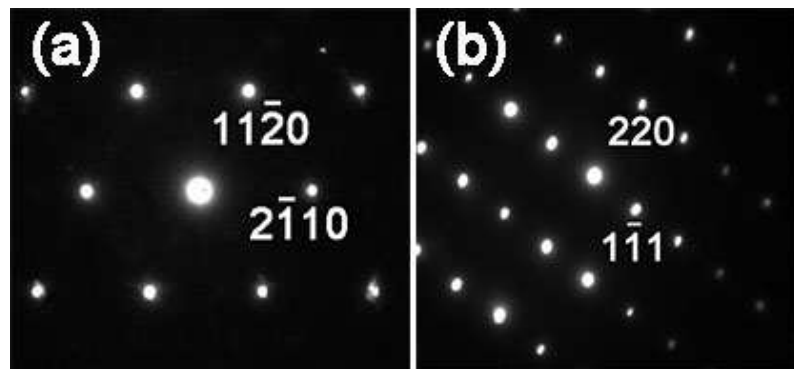


Fig.4 (a) and (b) Different SAED patterns corresponding to α -Fe₂O₃ and γ -Fe₂O₃

α -Fe₂O₃ and γ -Fe₂O₃ structures were observed at the same time depending on their SAED patterns. It is also mentioned and discussed by Cai *et al.* [5]. Fig.4a is taken along [0001] zone axis, which is indexed with α -Fe₂O₃ structure. And Fig.4b can be indexed with the γ -Fe₂O₃ structure,

which is taken along $[\bar{1}1\bar{2}]$ zone axis. Coexistence of α -Fe₂O₃ and γ -Fe₂O₃ may be depending on the changes of grain size and temperature but the real mechanism is still elusive [6]. α/γ transformation of Fe₂O₃ is also discussed in other literatures [7].

Depending on our investigations, compositions of different layers were clarified. From iron substrate to its surface, four different layers were identified as FeO, Fe₃O₄, Fe₂O₃ and Fe₂O₃ NWs. The ratios of Fe to O in different iron oxides are 1:1, 1:1.33 (3:4), 1:1.5 (2:3), respectively. It can be seen that the ratio of Fe to O decreases closing to the surface. The main reason why the ratio decreases is that oxygen content increases gradually closing to the surface and the content of iron ion is sufficient for different layers. On the basis of the observations, a possible mechanism of the oxidation of iron is proposed. As oxygen concentration increases closing to the surface, iron is oxidized to FeO firstly; and then FeO is oxidized to Fe₃O₄; finally, Fe₃O₄ is oxidized to Fe₂O₃ and Fe₂O₃ is the most stable iron oxide at ambient conditions.

Conclusions

In conclusion, it is revealed that there are four different layers from iron substrate to its surface, which is identified as FeO, Fe₃O₄, Fe₂O₃ and Fe₂O₃ NWs. The main reason that different layers consist of different iron oxides is the decrease of oxygen content with the increase of depth. Different iron oxide layers develop as oxygen concentration changes. Additionally, α -Fe₂O₃ and γ -Fe₂O₃ structures were observed at the same time but the reason of coexistence is still not clear.

Acknowledgement

This work was financially supported by the Program of Science and Technology for Higher Education in Shandong Province (Grant no.: J12LA17).

Reference

- [1] Q. Liu, Z.M. Cui, Z. Ma, S.W. Bian, W.G. Song, L.J. Wan, *Nanotechnology* 18, 385605 (2007)
- [2] L. Huo, W. Li, L. Lu, H. Cui, S. Xi, J. Wang, B. Zhao, Y. Shen, Z. Lu, *Chem. Mater.* 12, 790 (2000)
- [3] H. Srivastava, P. Tiwari, A.K. Srivastava, R.V. Nandedkar, *J. Appl. Phys.* 102, 054303 (2007)
- [4] X. Wang, R. Zhang, C. Wu, Y. Dai, M. Song, S. Gutmann, F. Gao, G. Lv, J. Li, X. Li, *J. Biomed. Mater. Res. A* 80, 852 (2006)
- [5] R. Cai, T. Li, Y. Wang, C. Wang, L. Yuan, G. Zhou, *J. Nanopart. Res.* 14, 1 (2012)
- [6] M. Multani, P. Ayyub, *Condens. Matter News* 1, 25 (1991)
- [7] T. Belin, N. Millot, N. Bovet, M. Gailhanou, *J. Solid State Chem.* 180, 2377 (2007)

Advances in Applied Science, Engineering and Technology

10.4028/www.scientific.net/AMR.709

Mechanism of the Oxidation of Iron

10.4028/www.scientific.net/AMR.709.106